Test Particle Methods

ISSS-15:International School/Symposium for Space Simulations
Garching, Germany

Patricio Muñoz[1], Jan Benáček[2]

[1]Center for Astronomy and Astrophysics, Technical University of Berlin
[2]Institute for Physics and Astronomy, University of Potsdam
Berlin/Potsdam, Germany

01st August 2024

Contents

Contents

Contents

Definitions

- Phase space: Multi-dimensional space consisting of all particle trajectories and momenta (velocities): $\vec{x}_1, \vec{p}_1, \vec{x}_2, \vec{p}_2, \cdots, \vec{x}_N, \vec{p}_N$
- Ensemble: Set of all microscopic state of a system consistent with given macroscopic parameters $(n, \vec{V}, P)$

Distribution function and phase space

- f: Probability density for finding any particle in the phase space volume element $[x, x + dx], [y, y + dy], [z, z + dz]$ and with velocities $[v_x, v_x + dv_x], [v_y, v_y + dv_y], [v_z, v_z + dv_z]$ such that:

$$d^6 N = f(\vec{x}, \vec{v}, t) \times d^3\vec{x} \times d^3\vec{v}$$

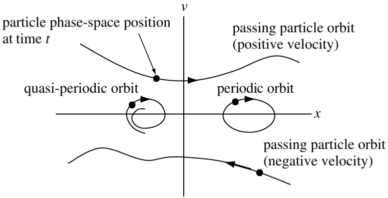

Figure 1: Trajectories in phase space

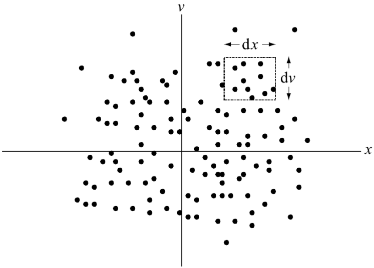

Figure 2: Volume element in phase space

Maxwell-Boltzmann distribution function

- The Maxwell-Boltzmann distribution represent the thermal equilibrium. It is a stationary and homogeneous solution of the kinetic equations.

$$f_\alpha = n_{0\alpha}\left(\frac{m_\alpha}{2\pi k_B T_\alpha}\right)^{3/2}\exp\left(-\frac{m_\alpha \vec{v}^2}{2k_B T_\alpha}\right)$$

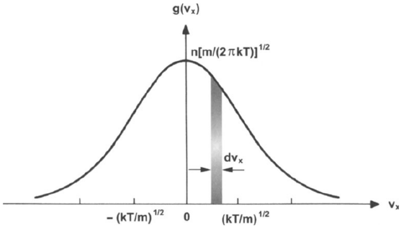

Figure 3: 1D Maxwellian

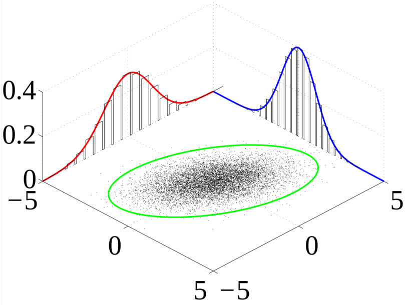

Figure 4: 2D anisotropic Maxwellian

Full equations of motion

Full equations of motion

$$\nabla \cdot \vec{E}(\vec{x}, t) = \frac{\rho(\vec{x}, t)}{\epsilon_0} \quad (1)$$

$$\nabla \cdot \vec{B}(\vec{x}, t) = 0 \quad (2)$$

$$\nabla \times \vec{E}(\vec{x}, t) = -\frac{\partial \vec{B}(\vec{x}, t)}{\partial t} \quad (3)$$

$$\nabla \times \vec{B}(\vec{x}, t) = \mu_0 \vec{J}(\vec{x}, t) + \mu_0 \epsilon_0 \frac{\partial \vec{E}(\vec{x}, t)}{\partial t} \quad (4)$$

$$\frac{dv_i}{dt} = \frac{q}{m}\left[\vec{E}(\vec{x}_i, t) + \vec{v} \times \vec{B}(\vec{x}_i, t)\right] \quad (5)$$

$$\rho(\vec{x}, t) = \sum_\alpha q_\alpha \int dv^3 \sum_i \delta(\vec{x} - \vec{x}_i)\delta(\vec{v} - \vec{v}_i) \quad (6)$$

$$\vec{J}(\vec{x}, t) = \sum_\alpha q_\alpha \int dv^3 \, \vec{v} \sum_i \delta(\vec{x} - \vec{x}_i)\delta(\vec{v} - \vec{v}_i) \quad (7)$$

But this approach is unpractical...

Vlasov equation 1

- Liouville's theorem: in *absence of collisions*, f is invariant following the motion in the 6D phase space.
  $\rightarrow$ Conservation of $f(\vec{x}, \vec{v}, t)$ in phase space: $df/dt = 0$
- Convective derivative: $d/dt = \partial/\partial t + \vec{v} \cdot \partial/\partial\vec{x} + \vec{a} \cdot \partial/\partial\vec{v}$
- Lorentz force: $\vec{a} = (q/m)\left(\vec{E} + \vec{v} \times \vec{B}\right)$

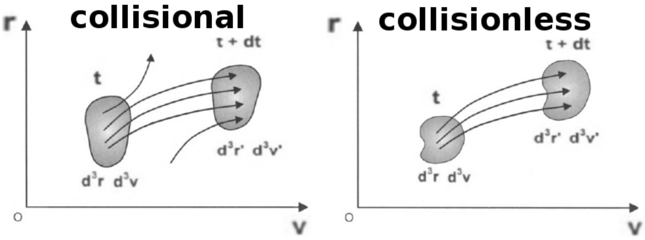

Figure 5: Collisions and conservation of phase space [Bittencourt, 2004]

Vlasov equation 2

- Note that here $\vec{E}$ and $\vec{B}$ are long-range averaged (in space and time) macroscopic fields from all the plasma particles and external sources (but no microscopic fields due to binary collisions).

Vlasov equation

$$\frac{df_\alpha(\vec{x},\vec{v},t)}{dt} = \left[\frac{\partial}{\partial t} + \vec{v}\cdot\frac{\partial}{\partial \vec{x}} + \frac{q_\alpha}{m_\alpha}\left(\vec{E}(\vec{x},t) + \vec{v}\times\vec{B}(\vec{x},t)\right)\cdot\frac{\partial}{\partial \vec{v}}\right] f_\alpha(\vec{x},\vec{v},t) = 0$$

Fully-kinetic/Vlasov description

Fully-kinetic equations

$$\nabla \cdot \vec{E} = \frac{\rho}{\epsilon_0} \quad (8)$$

$$\nabla \cdot \vec{B} = 0 \quad (9)$$

$$\nabla \times \vec{E} = -\frac{\partial \vec{B}}{\partial t} \quad (10)$$

$$\nabla \times \vec{B} = \mu_0 \vec{J} + \mu_0 \epsilon_0 \frac{\partial \vec{E}}{\partial t} \quad (11)$$

$$\left[\frac{\partial}{\partial t} + \vec{v} \cdot \frac{\partial}{\partial \vec{x}} + \frac{q_\alpha}{m_\alpha} \left(\vec{E} + \vec{v} \times \vec{B}\right) \cdot \frac{\partial}{\partial \vec{v}}\right] f_\alpha = 0 \quad (12)$$

$$\rho = \sum_\alpha q_\alpha \int dv^3 \, f_\alpha \quad (13)$$

$$\vec{J} = \sum_\alpha q_\alpha \int dv^3 \, \vec{v} f_\alpha \quad (14)$$

How to solve the Vlasov/plasma equation

- Fluid/MHD: Solve for moments of f_α ($\int v^n d^3\vec{v}$ (Vlasov eq.). $n = 0$: density, $n = 1$: momentum, $n = 2$: energy/pressure/temperature)
- Vlasov: Solve for f_α directly
- Simulate particles sampling f_α:
    - Particle-particle methods (N-body): scaling as N^2
    - PIC scales as $\sim N$
- Hybrid models: part kinetic/Vlasov, part fluid.
- Test particle methods: another way to bridge the gap between fluids and kinetic models, providing first-order estimates of kinetic effects in problems for which a fully-kinetic solution is not practical.

Hierarchy of plasma physics models

- Kinetic description: microscopic properties, it uses the velocity distribution function f.
- Fluid description: it uses a few macroscopic quantities, averages of the distribution function (mean velocity, pressure/temperature). Valid for or near thermodynamic equilibrium.

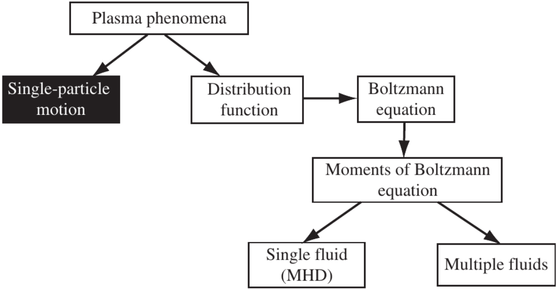

Figure 6: Hierarchy of plasma physics models

The test particle method

1. Obtain electromagnetic fields $\vec{E}$, $\vec{B}$ from another methods or observations (decoupling Maxwell equations).
2. Integrate particle trajectories using those electromagnetic fields via, e.g.,
    1. Full Lorentz force:

$$\frac{dv_i}{dt} = \frac{q}{m}\left[\vec{E}(\vec{x}_i, t) + \vec{v} \times \vec{B}(\vec{x}_i, t)\right] \tag{15}$$

    2. Guiding center approximation.
3. Use the trajectories to infer approximate kinetic properties of the system.

Note that this approach is not self-consistent, the particles do not have any effect on the fields (no feedback or corrections).

Contents

Contents

Particle motion in background magnetic fields

- The basic motion of a particle under the influence of a static and uniform magnetic field is the gyromotion.
- Taking the dot product of Eq. (15) with $\vec{v}$, we get

$$\frac{d}{dt}\left(\frac{mv^2}{2}\right) = 0$$

i.e., a static magnetic field cannot change the kinetic energy of a particle.

- Assuming a magnetic field $\vec{B} = B\hat{z}$, Eq. (15) becomes:

$$m\frac{dv_x}{dt} = qBv_y \quad (16)$$

$$m\frac{dv_y}{dt} = -qBv_x \quad (17)$$

$$m\frac{dv_z}{dt} = 0 \quad (18)$$

and thus,

$$\frac{d^2 v_x}{dt^2} + \Omega_c^2 v_x = 0 \quad (19)$$

$$\frac{d^2 v_y}{dt^2} + \Omega_c^2 v_y = 0 \quad (20)$$

Particle motion in background magnetic fields

- Where the gyrofrequency (or Larmor/cyclotron) is:

$$\Omega_c = \frac{qB}{m} \tag{21}$$

- Solution

$$v_x = v_\perp \cos(\Omega_c t + \psi) \tag{22}$$

$$v_y = v_\perp \sin(\Omega_c t + \psi) \tag{23}$$

$$v_z = v_\parallel \tag{24}$$

where ψ is an arbitrary phase angle.

- By integrating we get,

$$x = \rho_c \sin(\Omega_c t + \psi) + (x_0 - r_c \sin\psi) \tag{25}$$

$$y = -\rho_c \cos(\Omega_c t + \psi) + (y_0 + r_c \cos\psi) \tag{26}$$

$$z = z_0 + v_\parallel t \tag{27}$$

Particle motion in background magnetic fields

- Where the gyroradius (or Larmor radius or cyclotron radius) is:

$$\rho_c = \frac{|v_\perp|}{\Omega_c} = \frac{m|v_\perp|}{|q|B} \tag{28}$$

Note that this can be understood from force balancing the "centrifugal" force:

$$\frac{mv_\perp^2}{r} = qv_\perp B \tag{29}$$

- Particles move in circular/helical orbits with frequency Ω_c and radius ρ_c about the guiding center $R_g = \hat{x}x_0 + \hat{y}y_0 + \hat{z}(z_0 + v_\parallel t)$
- Note that particles with higher velocities orbit in circles with larger radii, but same frequency.
- Particles with larger masses orbit in circles with larger radii, but with lower frequencies (longer periods).

Particle motion in magnetic fields

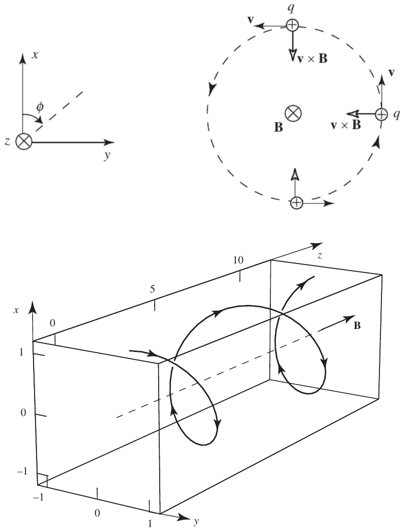

Particle motion in background magnetic fields

- Pitch angle:

$$\alpha = \tan^{-1}\left(\frac{v_\perp}{v_\parallel}\right) \tag{30}$$

- Magnetic moment

$$\mu = \underbrace{\frac{q\Omega_c}{2\pi}}_{\text{current}} \underbrace{\pi\rho_c^2}_{\text{area}} = \frac{mv_\perp^2}{2B} \tag{31}$$

- The direction of the magnetic field generated by the gyration is opposite to that of the external field: a plasma is a diamagnetic medium.

Contents

$\vec{E} \times \vec{B}$ drift

- Let us consider, in addition to $\vec{B} = \hat{z}B$, an electric field: $\vec{E} = \hat{x}E_\perp + \hat{z}E_\parallel$. The equations of motions are:

$$m\frac{d\vec{v}_\perp}{dt} = q(\hat{x}E_\perp + \vec{v}_\perp \times \hat{z}B) \tag{32}$$

$$m\frac{dv_\parallel}{dt} = qE_\parallel \tag{33}$$

- Let us decompose $\vec{v}_\perp = \vec{v}_E + \vec{v}_{ac}$. By choosing:

$$\vec{v}_E = \frac{\vec{E} \times \vec{B}}{B^2} \tag{34}$$

Eq. (32) becomes the eq. for gyration with frequency Ω_c.

$$m\frac{d\vec{v}_{ac}}{dt} = q\vec{v}_{ac} \times \hat{z}B \tag{35}$$

- The solution is then:

$$\vec{v}(t) = \hat{z}v_\parallel(t) + \vec{v}_E + \vec{v}_{ac}(t) \tag{36}$$

$\vec{E} \times \vec{B}$ drift

- The average of $\vec{v}$ over one gyroperiod is:

$$\langle \vec{v} \rangle = \hat{z} v_{\parallel} + \vec{v}_E \tag{37}$$

so $\vec{v}_E$ is the average perpendicular velocity.
- This drift arises from the difference in the local gyroradius between top/bottom.
- The $\vec{E} \times \vec{B}$ drift is independent on q, m and $v_{\perp}$.

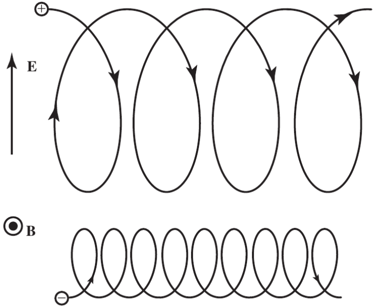

Gradient B drift

- Let us assume a magnetic field with intensity varying in the perpendicular direction to the B-vector $\vec{B}(y) = \hat{z}B_z(y)$.
- This drift also arises from a force perpendicular to the magnetic field. Generalizing the expression for the $\vec{E} \times \vec{B}$ force:

$$\vec{v}_F = \frac{(\vec{F}_\perp/q) \times \vec{B}}{B^2} \tag{38}$$

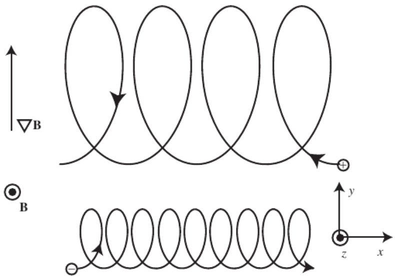

Gradient B drift

- In this geometry, the perpendicular force is

$$\vec{F} = q\vec{v} \times \vec{B} = \hat{x} q v_y B_z - \hat{y} q v_x B_z \quad (39)$$

$$\sim \hat{x} q v_y \left(B_0 + y \frac{\partial B_z}{\partial y} \right) - \hat{y} q v_x \left(B_0 + y \frac{\partial B_z}{\partial y} \right) \quad (40)$$

- By assuming that particles follow approximately orbits in an uniform field (Eqs. (25)-(26)), we can determine the gyroaverage force $\vec{F}$:

$$\langle F_y \rangle = \frac{q v_\perp r_c}{2} \frac{\partial B_z}{\partial y} = \frac{m v_\perp^2}{2B} \frac{\partial B_z}{\partial y} \quad \text{or more generally} \quad = \frac{W_\perp}{B} \nabla B \quad (41)$$

- This way, the grad-B ($\nabla \vec{B}$) drift velocity is:

$$\vec{v}_\nabla = \frac{(\vec{F}_\perp / q) \times \vec{B}}{B^2} = \frac{\langle \vec{F}_y \rangle \hat{y} \times \hat{z} B_z}{q B_z^2} \quad (42)$$

$$= \frac{m v_\perp^2}{2 q B_z} \frac{\partial B_z}{\partial y} \hat{x} \quad \text{or more generally} \quad = \frac{m v_\perp^2}{2q} \frac{\vec{B} \times \nabla B}{B^3} \quad (43)$$

Curvature B drift

- In a curved magnetic field line, particles experience a centrifugal force perpendicular to the B-field

$$\vec{F}_{cf} = m v_{\parallel}^2 \frac{\vec{R}_c}{R_c^2} \quad (44)$$

which causes a drift perpendicular to both vectors.

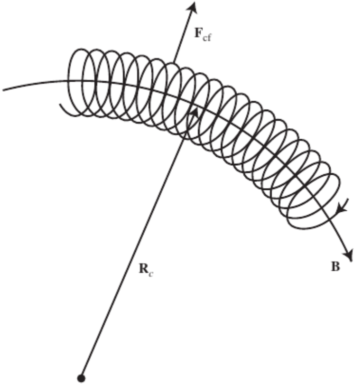

Curvature B drift

- Curvature drift:

$$\vec{v}_R = \frac{(\vec{F}_{cf}/q) \times \vec{B}}{B^2} = \tag{45}$$

$$= \frac{m v_\parallel^2}{q} \frac{\vec{R}_c \times \vec{B}}{R_c^2 B^2} \tag{46}$$

- In vacuo this drift cannot be the only one because $\nabla \times \vec{B} = 0$. A more general expression due to both gradient and curvature drifts is:

$$\vec{v}_{total} = \vec{v}_R + \vec{v}_\nabla = \left(v_\parallel^2 + v_\perp^2/2\right) \frac{\vec{B} \times \nabla B}{\Omega_c B^2} \tag{47}$$

Curvature B drift

- Longitudinal drift of radiation belt electrons (and associated ring current because of opposite ion/electron drift)

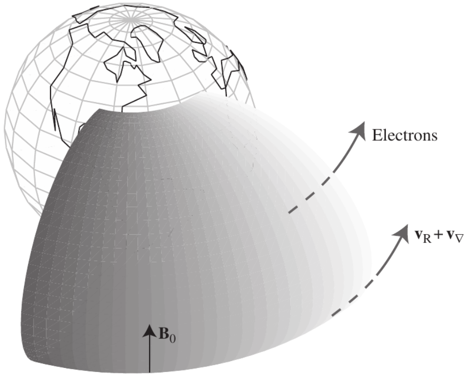

Adiabatic invariance of the magnetic moment

- Magnetic moment $\mu = \frac{mv_\perp^2}{2B}$ tends to be conserved as long as (spatial or temporal) changes in B are small over a gyroradius or gyroperiod.
- The particle's perpendicular energy increases while its parallel energy decreases as it moves toward regions of stronger B, until it eventually reaches $v_\parallel = 0$ and it bounces back (magnetic mirror/bottle).

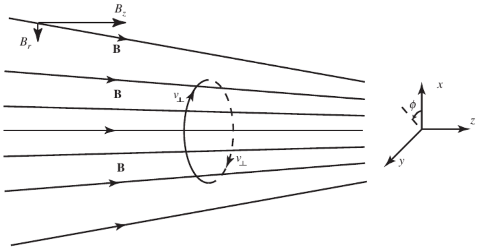

Polarization drift

- In a slowly varying electric field the so-called polarization drift appears:

$$\vec{v}_p = \frac{m}{qB^2}\frac{d\vec{E}}{dt} \quad (48)$$

- This drift depends on the particles' mass and charge, and it can change the particle's energy.

Contents

Guiding center approximation

- Valid when the gyroradius ($\rho = mv/qB$) and gyroperiod ($\propto 1/\Omega = m/qB$) are much smaller than the length scale of transverse gradients and characteristic oscillation periods of the background EM fields
- The motion of a charged particle is described in terms of variables representing the gyration around B-field lines and the motion of its guiding center.
- For the solar corona, typical gyroradii are $10^{-3}m$ for electrons and $10^{-2}m$ for protons, much smaller than typical characteristic lengths scales.

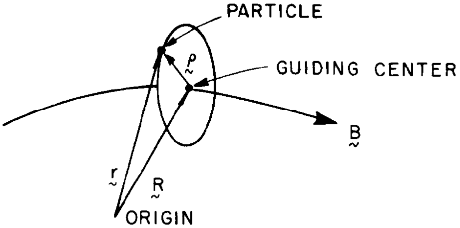

Guiding center approximation

- Non-relativistic version [Northrop, 1963]:

$$\frac{d\vec{R}}{dt} = v_{\parallel}\hat{b} + \frac{\hat{b}}{B} \times \left(-\vec{E} + \frac{m}{q}\left(v_{\parallel}\frac{d\hat{b}}{dt} + \frac{d\vec{v}_E}{dt} \right) + \frac{\mu}{q}\nabla B \right) \quad (49)$$

$$\frac{d(mv_{\parallel})}{dt} = m\vec{u}_E \cdot \frac{d\hat{b}}{dt} + qE_{\parallel} - \mu\hat{b}\cdot\nabla B \quad (50)$$

with: $\vec{R}$: guiding center position, $\hat{b}$ unit vector along the B-field, $\vec{v}_E = \vec{E}\times\hat{b}/B$ is the $\vec{E}\times\vec{B}$ drift velocity and $\mu = mv_{\perp}^2/2B$ is the magnetic moment.

- In Eq. (49). 1st term: parallel motion, 2nd term: $\vec{E}\times\vec{B}$ drift, 3rd term: curvature drift, 4st term: polarization drift, 5th is the gradient-B drift.

Contents

Contents

2nd-order Runge-Kutta

- It is based on the exact integration of $dy/dt = f(t, y)$

$$y_{i+1} = y_i + \int_{t_i}^{t_{i+1}} f(t, y)dt \qquad (51)$$

- The basis for RK2 is to approximate $f(t, y)$ by a Taylor expansion w/r to the middle point:

$$f(t, y) \approx f(t_{i+1/2}, y_{i+1/2}) + (t - t_{i+1/2}) \left.\frac{df}{dt}\right|_{t_{i+1/2}}$$

- Since the integral of the 2nd term vanishes,

$$y_{i+1} = y_i + hf(t_{i+1/2}, y_{i+1/2}) + \mathcal{O}(h^3)$$

- Finally, the value of $y_{i+1/2}$ is obtained by the Euler's method: $y_{i+1/2} \approx y_i + \frac{h}{2} f(t_i, y_i)$.

2nd-order Runge-Kutta (RK2)

$$y_{i+1} = y_i + k_2$$
$$k_1 = hf(t_i, y_i)$$
$$k_2 = hf(t_i + \frac{h}{2}, y_i + \frac{k_1}{2})$$

- The local/global error is $\mathcal{O}(h^3)/\mathcal{O}(h^2)$.
- Here $h = \Delta t$

Runge-Kutta methods: General derivation

- The family of Runge-Kutta methods are derived from the following Taylor expansion, without explicit calculation of the derivatives:

$$y(t_{i+1}) = y(t_i + h) = y(t_i) + hy'(t_i) + \frac{h^2}{2}y''(t_i) + \cdots$$

- In particular, RK2 is obtained by finding the constants a_1, a_2, p_1, q_{11} such as the following formula coincides with the Taylor expansion to 2nd order:

$$\begin{aligned} y_{i+1} &= y_i + a_1 k_1 + a_2 k_2, \quad \text{con} \\ k_1 &= hf(t_i, y_i) \\ k_2 &= hf(t_i + p_1 h, y_i + q_{11} k_1 h) \end{aligned}$$

- The solution is:

$$a_1 + a_2 = 1, \qquad a_2 p_1 = \frac{1}{2}, \qquad a_2 q_{11} = \frac{1}{2}$$

- Since there are 3 eqs but 4 unknowns, there is some freedom of choice- By choosing $a_2 = 1/2$, we get the (improved) Euler's method. Choosing $a_2 = 1$, we get RK2 with $a_1 = 0$, $p_1 = 1/2$, $q_1 = 1/2$.

4th-order Runge Kutta

- By considering more terms in the Taylor expansion, it is possible to improve the precision of RK2. The most popular algorithm (since the XIX century) is:

4th-order Runge Kutta (classic RK, RK4)

$$y_{i+1} = y_i + \frac{1}{6}(k_1 + 2k_2 + 2k_3 + k_4)$$
$$k_1 = hf(t_i, y_i)$$
$$k_2 = hf(t_i + \frac{h}{2}, y_i + \frac{k_1}{2})$$
$$k_3 = hf(t_i + \frac{h}{2}, y_i + \frac{k_2}{2})$$
$$k_4 = hf(t_i + h, y_i + k_3)$$

- Global/local error $\mathcal{O}(h^5)/\mathcal{O}(h^4)$
- RK4 estimates the value of y_{i+1} by averaging 4 slopes
- It provides a good balance between accuracy and computational cost

4th-order Runge Kutta

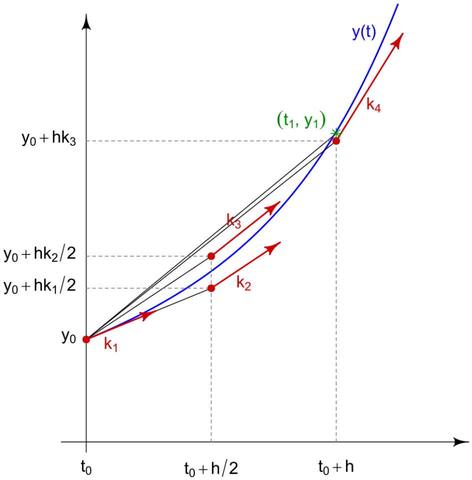

Figure 7: Slopes used for the Runge-Kutta method

4th-order Runge Kutta

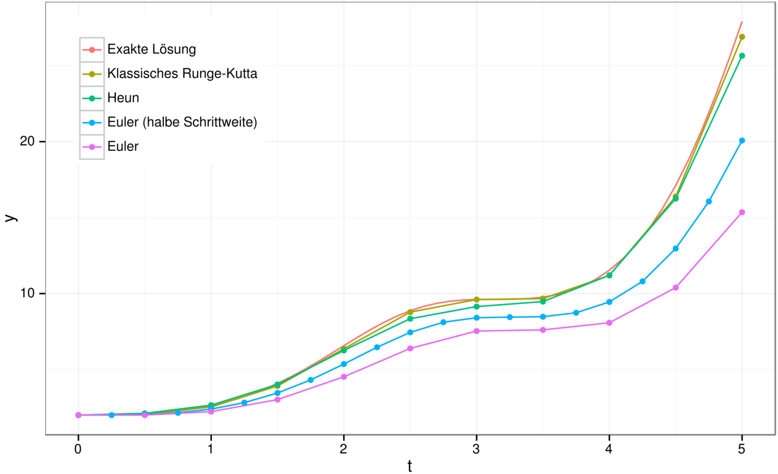

Figure 8: Comparison of Runge-Kutta with other methods for the solution of the ODE: $y' = sin^2(t) * y$

Contents

Symplectic methods

- When we apply conventional methods like Euler's or RK to a Hamiltonian system, it causes an artificial excitation or damping.
- For autonomous Hamiltonian systems:

$$\frac{dq}{dt} = \frac{\partial H}{\partial p}, \quad \frac{dp}{dt} = -\frac{\partial H}{\partial q}$$

  H is conserved and the two-form $dp \wedge dq =$ constant (Jacobian)
- A numerical integration scheme satisfying those two properties is symplectic, they preserve the phase space density. They conserve the energy (time-reversible).
- Assuming known the Hamiltonian ($\sim$ energy) of the system, symplectic methods can be written by an n-iteration of:

$$x_i = x_{i-1} + c_i \Delta t \, x_{i-1} \tag{52}$$

$$v_i = v_{i-1} + d_i \Delta t \, a(x_i) \tag{53}$$

  where $a = F/m$ and c_i, d_i are constants.
- There are explicit symplectic algorithms for separable Hamiltonians: $H = T(p) + V(q)$ (conservative systems). Note that unfortunately the Hamiltonian of charged particles in EM fields is not separable: $H(\vec{p}, \vec{x}) = (1/2)(\vec{p} - \vec{A})^2 + \phi$. More info: [Yoshida, 1993]

Verlet's algorithm

- Example for the 2nd Newton's law: using a finite central difference of 2nd order for $d^2x/dt^2 = F/m = a$, and central difference for the first derivative $dx/dt = v$
- Thus, we get an algorithm very useful for N-body problems, which is also symplectic: $c_1 = c_2 = 1/2$, $d_1 = 1$, $d_2 = 0$.

Verlet's (Störmer) algorithm

$$\vec{x}_{i+1} = 2\vec{x}_i - \vec{x}_{i-1} + (\Delta t)^2 \vec{a}_i + \mathcal{O}(\Delta t)^4$$

$$\vec{v}_i = \frac{1}{2\Delta t}\left(\vec{x}_{i+1} - \vec{x}_{i-1}\right) + \mathcal{O}(\Delta t)^2$$

- The local/global error is $\mathcal{O}(h^4)/\mathcal{O}(h^2)$.
- Initialization: multistep method: 2 initial positions are required: $\vec{x}_0$ y $\vec{x}_1$, but we have only the initial conditions $\vec{x}_0$ y $\vec{x}_0$. We can assume $\vec{F} = constant$ in the first interval $[0, \Delta t]$, so that we can use $\vec{x}_1 \approx \vec{x}_0 + \Delta t \vec{v}_0 + \vec{a}_0 \Delta t^2/2$

Velocity Verlet

- 2nd-order method, where $\vec{v}$ and $\vec{x}$ are simultaneously calculated. Similar standard Verlet. Algorithm:
  1. $\vec{v}_{n+1/2} = \vec{v}_n + \vec{a}_n \Delta t/2$ (constant coordinates)
  2. $\vec{x}_{n+1} = \vec{x}_n + \vec{v}_{n+1/2}\Delta t = \vec{x}_n + \vec{v}_n \Delta t + \vec{a}_n \Delta t^2/2$ (constant velocities)
  3. $\vec{a}_{n+1} = \vec{a}(\vec{x}_{n+1}, t_{n+1})$
  4. $\vec{v}_{n+1} = \vec{v}_{n+1/2} + \vec{a}_{n+1}\Delta t/2 = \vec{v}_n + (\Delta t/2)(\vec{a}_n + \vec{a}_{n+1})$ (constant coordinates)
- Advantage over classical Verlet: only one initial value for $\vec{x}$ and $\vec{v}$ are needed, less round-off errors

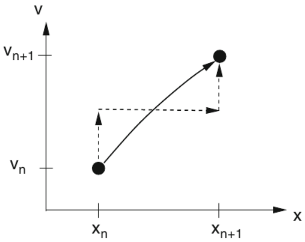

Leapfrog method

- 2nd-order symplectic method where $\vec{x}$ and $\vec{v}$ are calculated alternatively ($\vec{x}$ in multiples of Δt and velocities in half-integer multiples of Δt). Otherwise is similar to velocity Verlet. It is equivalent to use different grids for $\vec{x}$ and $\vec{v}$, shifted in $\Delta t/2$.
  1. $\vec{v}_{n+1/2} = \vec{v}_{n-1/2} + \vec{a}_n \Delta t$ (constant $\vec{x}$)
  2. $\vec{x}_{n+1} = \vec{x}_n + \vec{v}_{n+1/2} \Delta t$ (constant $\vec{v}$)

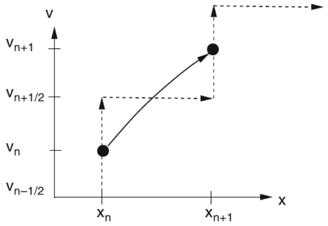

Boris algorithm

- Specifically used to advance particles in plasma simulations (it is the *de facto* algorithm).
- It has very good conservation properties: it conserves phase space volume, even though it is not symplectic [Qin et al., 2013]
- Discretized Lorentz force:

$$\frac{\vec{x}^{i+1/2} - \vec{x}^{i-1/2}}{\Delta t} = \vec{v}^{i+1} \tag{54}$$

$$\frac{\vec{u}^{i+1} - \vec{u}^{i}}{\Delta t} = \frac{q}{m}\left(\vec{E}^{i} + \frac{(\vec{v}^{i+1} + \vec{v}^{i})}{2} \times \vec{B}^{i}\right) \tag{55}$$

  with $\vec{u} = \gamma\vec{v}$. Note in the RHS of the acceleration eq. the average velocity $(\vec{v}^{i+1} + \vec{v}^{i})/2 = \vec{v}^{i+1/2}$

- The idea of the Boris algorithm is to separate the electric and magnetic force in 3 parts: first half of the electric force is determined, then the full magnetic force (rotation) and finally the second half of the electric force.

Boris push

1. $$\vec{u}^{-} = \vec{u}^{i} + \frac{q\Delta t}{2m}\vec{E}^{i+1/2}$$

2. $$\frac{\vec{u}^{+} - \vec{u}^{-}}{\Delta t} = \frac{q}{m}\left(\vec{v}^{i+1/2} \times \vec{B}^{i+1/2}\right)$$

3. $$\vec{u}^{i+1} = \vec{u}^{+} + \frac{q\Delta t}{2m}\vec{E}^{i+1/2}$$

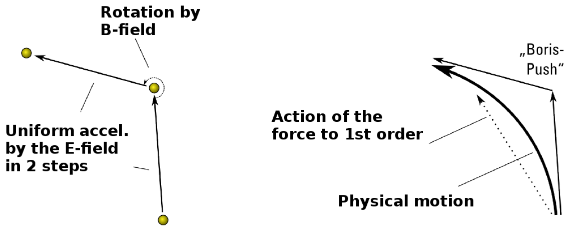

Figure 9: Boris push

Boris push

- The phase angle of the rotation (2nd part):

$$\theta = \frac{q\Delta t}{m\gamma^-} B^{i+1/2} \tag{56}$$

- The rotation is solved in this way:

$$\vec{u}' = \vec{u}^- + \vec{u}^- \times \vec{t} \tag{57}$$

$$\vec{u}^+ = \vec{u}^- + \frac{2}{1+t^2}(\vec{u}' \times \vec{t}) \tag{58}$$

with

$$\vec{t} = \tan(\theta/2)\vec{b}^{i+1/2} \tag{59}$$

- Sometimes the previous equation is approximated as $\vec{t} = (\theta/2)\vec{b}$ (see a comparison in [Ripperda et al., 2018, Zenitani and Umeda, 2018])

Boris algorithm

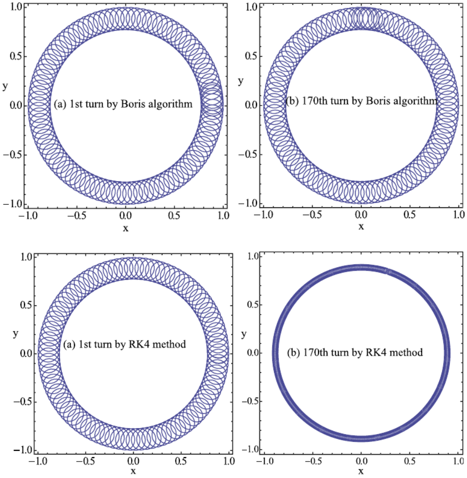

Figure 10: Comparison of trajectories in a given B-field between RK4 and Boris algorithms [Qin et al., 2013]

Boris algorithm

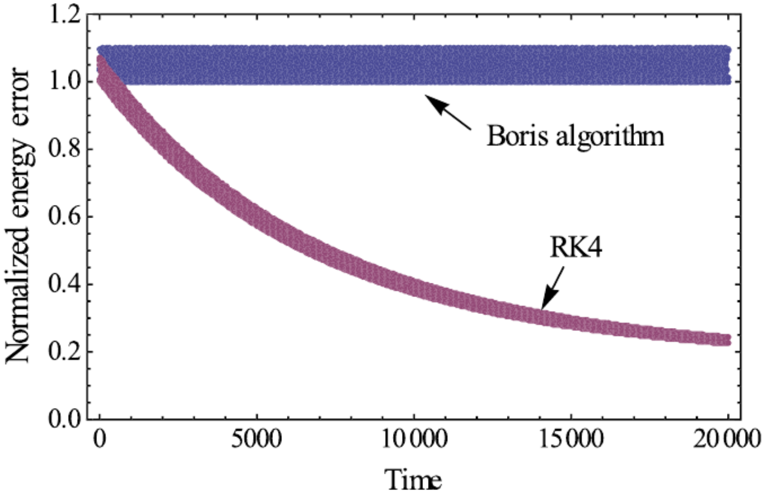

Figure 11: Comparison of energies of a charged particle moving in a given B-field, with its trajectory calculated using the RK4 and Boris algorithms [Qin et al., 2013]

Vay pusher

- Another particle pusher specifically developed for relativistic particles [Vay, 2008].
- It is based on a modification of the Boris algorithm that is designed to avoid spurious perpendicular electric fields due to the relativistic Lorentz transformation of the EM-fields.
- It preserves the $\vec{E} \times \vec{B}$ velocity (regardless the value of Δt), also in the relativistic case, so it has attracted attention for applications to laser-plasma interactions and relativistic astrophysics.
- It does not conserve the phase space volume.

Vay pusher

- In the part 2 (rotation) of the Boris algorithm, the average velocity is calculated as:

$$\vec{v}^{i+1/2} = \frac{\gamma^i \vec{v}^i + \gamma^{i+1} \vec{v}^{i+1}}{2\gamma^{i+1/2}} \tag{60}$$

with

$$\gamma^{i+1/2} = \sqrt{1 + \left(\gamma^i \vec{v}^i + \frac{q\Delta t}{2m} \vec{E}^{i+1/2}\right)} \tag{61}$$

- In the Vay's algorithm, this average is instead calculated as:

$$\vec{v}^{i+1/2} = \frac{\vec{v}^i + \vec{v}^{i+1}}{2} \tag{62}$$

which comes from considering the special case $\vec{E} + \vec{v} \times \vec{B} = 0$ in the original Boris algorithm, and leads to the rotation step:

$$\frac{\gamma^{i+1} \vec{v}^{i+1} - \gamma^i \vec{v}^i}{\Delta t} = \frac{q}{m} \left(\vec{E}^{i+1/2} + \vec{v}^{i+1/2} \times \vec{B}^{i+1/2}\right) \tag{63}$$

whose solution leads to a two-step procedure for $\vec{u}^{i+1/2}$ and then $\vec{u}^i$ (with $\vec{u}^i = \gamma^i \vec{v}^i$ [Vay, 2008]

Vay vs Boris pushers

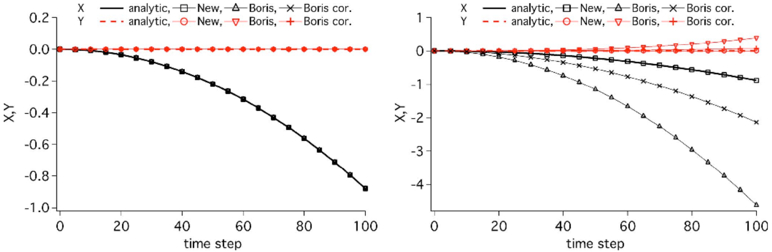

FIG. 2. (Color online) X and Y positions vs time step of a particle accelerated by a constant electric field E_x as computed in the laboratory (left) or in a frame moving along $\hat{y}$ at $\gamma_f = 100$ (right).

Figure 12: [Vay, 2008]

Vay vs Boris pushers

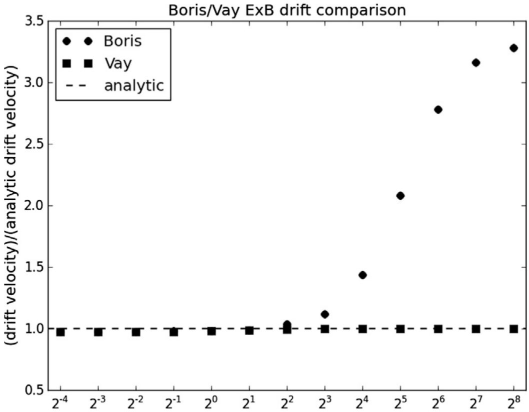

Fig. 6. $E \times B$ drift motion for the Vay and Boris movers as a function of $\omega_c \Delta t$. The y-axis gives the ratio of the drift velocity measured in the simulation to the analytic drift velocity.

Figure 13: [Belyaev, 2015]

Contents

Contents

The test particle method

1. Obtain electromagnetic fields $\vec{E}$, $\vec{B}$ from another methods or observations (decoupling Maxwell equations).
2. Integrate particle trajectories using those electromagnetic fields via, e.g.,
    1. Full Lorentz force:

$$\frac{dv_i}{dt} = \frac{q}{m}\left[\vec{E}(\vec{x}_i, t) + \vec{v} \times \vec{B}(\vec{x}_i, t)\right] \tag{64}$$

    2. Guiding center approximation.
3. Use the trajectories to infer approximate kinetic properties of the system.

Note that this approach is not self-consistent, the particles do not have any effect on the fields (no feedback or corrections).

- There are 4 formulations of the test particle method [Marchand, 2010, Voitcu et al., 2012]

Method 1: trajectory sampling

- It solves individual representative trajectories (the choice is not trivial)
- Useful to visualize aspects such as particle transport or energetics

Method 1: trajectory sampling

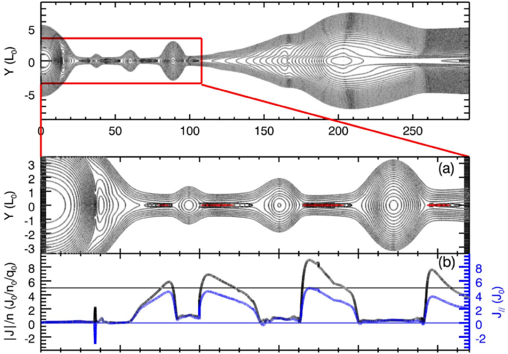

Figure 14: Magnetic reconnection simulation data [Zhou et al., 2016]

Method 1: trajectory sampling

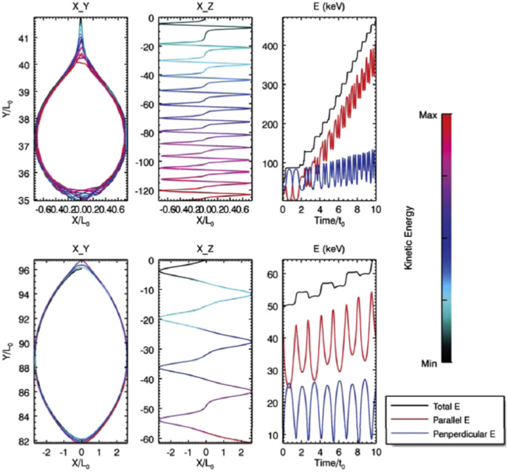

Figure 15: Particle trajectories [Zhou et al., 2015]

Method 2: Forward Monte Carlo

- Inject (randomly) particles in source regions where f is known, and follow them until they reach the regions of interest.
- Injected particles are tagged with a statistical weight w_i based on the number of injected particles per time Γ_{MC} and the physical flux Γ_{Phys}:

$$w_i = \frac{\Gamma_{Phys}}{\Gamma_{MC}}$$

- Statistical analysis of particles via sampling (binning) in x and v space (which implies large statistical errors), and using w_i. For instance:

$$n = \frac{1}{\Delta x^3} \sum_i^N w_i \tag{65}$$

$$\Gamma_x = \frac{1}{\Delta x^3} \sum_i^N v_{ix} w_i \tag{66}$$

$$f(\vec{x}, \vec{v}) = \frac{1}{\Delta x^3 \Delta v^3} \sum_i^N w_i \tag{67}$$

- It is the most similar approach to the PIC method, but with non self-consistent fields.

Method 2: Forward Monte Carlo

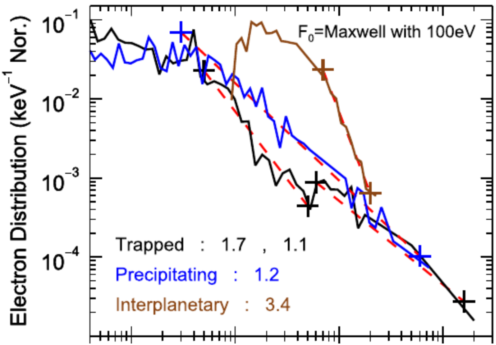

Figure 16: Final energy spectra [Zhou et al., 2016]

Method 3: Forward Liouville

- It makes use of the Liouville's theorem for f (i.e: only valid for the Vlasov eq.)
- Sampling is only in $\vec{x}$ space, implying smaller statistical errors.
- Procedure is similar as Forward Monte Carlo, except for
  - Particles are tagged with the value of f at the injection point.
  - Momenta of f are computed using the scattered representation of f
  - f can be interpolated onto a structured grid
- Within a spatial bin, the distribution of $\vec{v}_i$ is irregular, a unstructured grid and interpolation are required

Method 3: Forward Liouville

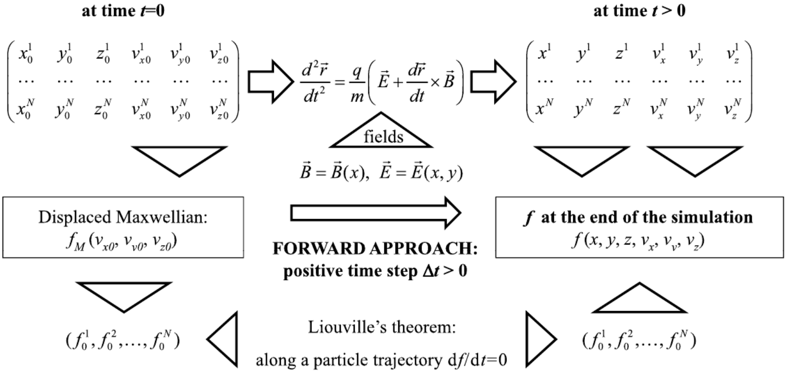

Figure 17: Forward Liouville scheme [Voitcu et al., 2012]

Method 4: Backward Liouville

- It also makes use of the Liouville's theorem for f (i.e: only valid for the Vlasov eq.)
- No sampling: neither in $\vec{x}$ nor in $\vec{v}$ space, implying no statistical errors (other than finite discretization or due to fields).
- The procedure starts by choosing a given point $\vec{x}$ in space, choosing a grid in velocity space at which f will be computed.
- From each velocity $\vec{v}_i$ in the grid, particle trajectories are integrated backwards in time.
- When particles reach the source region at $\vec{X}$ with velocity $\vec{V}_i$, the VDF is set as $f(\vec{x}, \vec{v}_i) = f(\vec{X}, \vec{V}_i)$

Method 4: Backward Liouville

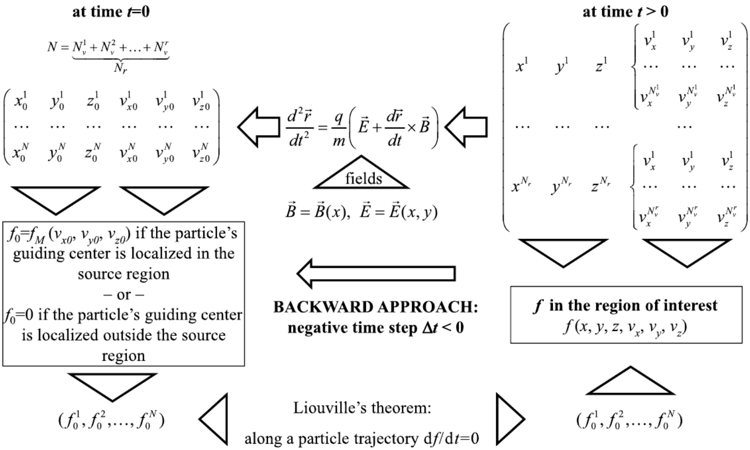

Figure 18: Backward Liouville scheme [Voitcu et al., 2012]

Contents

Contents

Exercises

- Exercise 1: Basic particle motion
- Exercise 2: Particles trajectories in magnetic reconnection
- Both can be executed from your browser on the following JupyterHub link: `https://notebooks.mpcdf.mpg.de/isss`
- The JupyterHub is based on a gitlab repository hosted at: `https://gitlab.mpcdf.mpg.de/munozp/test-particle-code-isss-14`
- Memory limit 4 Gb per notebook.
- Please stop the server before closing the browser tab. This can be found under: File −> Hub Control Panel −> Stop My Server

Exercise 1: Basic particle motion

- Investigate how various pushers impact the precision of the Larmor motion in the magnetic field.
- Investigate various particle drifts.
- How the size of time step dt influences the precision of particle position?
- Which of the particle pushers is the most precise?

Exercise 2: Particles in magnetic reconnection

- MHD simulation of magnetic reconnection (plasmoid/long current sheet).
- Physical model: Resistive MHD + subgrid-scale turbulent model.
- Parameters applied to Mercury's magnetotail
- Details in [Zhou et al., 2018], also at `https://arxiv.org/abs/1806.10665`

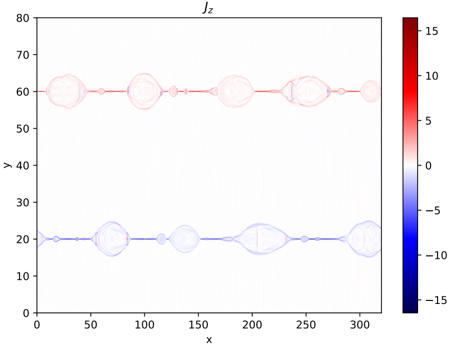

Figure 19: Out-of-plane current density j_z of the MHD simulation [Zhou et al., 2018]

Exercise 2: Particles in magnetic reconnection

- Simple python code
  1. read electromagnetic field data from MHD simulation snapshot (grid: $12802x3202$)
  2. compute supplementary fields (like current density)
  3. calculate electromagnetic fields at particles' position (interpolation)
  4. integrate particles using Lorentz force (TODO: guiding center approximation) eq via Runge-Kutta 4th order (TODO: Boris pusher)
  5. diagnostics (plots)
- Normalizations, $t_0 = 1s$, $B_0 = 7.5x10^{-8}T$, $L_0 = 2.5x10^4 m$, $\beta_p = 0.5$
- Integration parameters: $dt = 0.13\Omega_{ce}^{-1}$ $(10^{-5}t_0)$, $t_{max} = 3t_0$.

Exercise 2: Particles in magnetic reconnection

- Determine locations where particle acceleration occurs and the physical reasons (which field or drifts are responsible for it)
- Compute electron trajectories on the current sheet and plasmoids (put all particles at the same initial position, varying only the velocities)
- Use protons instead of electrons
- Use different solvers, such as the Boris pusher instead of RK4.

The end

Thank you for your attention

Questions/Comments?

Bibliography I

Belyaev, M. A. (2015).
PICsar: A 2.5D axisymmetric, relativistic, electromagnetic, Particle in Cell code with a radiation absorbing boundary.
New Astron., 36:37–49.

Bittencourt, J. (2004).
Fundamentals of Plasma Physics.
Springer.

Marchand, R. (2010).
Test-particle Simulation of Space Plasmas.
Commun. Comput. Phys., 8(3):471–483.

Northrop, T. G. (1963).
Adiabatic charged-particle motion.
Rev. Geophys., 1(3):283.

Qin, H., Zhang, S., Xiao, J., Liu, J., Sun, Y., and Tang, W. M. (2013).
Why is Boris algorithm so good?
Phys. Plasmas, 20(8):084503.

Ripperda, B., Bacchini, F., Teunissen, J., Xia, C., Porth, O., Sironi, L., Lapenta, G., and Keppens, R. (2018).
A Comprehensive Comparison of Relativistic Particle Integrators.
Astrophys. J. Suppl. Ser., 235(1):21.

Vay, J. L. (2008).
Simulation of beams or plasmas crossing at relativistic velocity.
Phys. Plasmas, 15:056701.

Bibliography II

Voitcu, G., Echim, M., and Marchand, R. (2012).
Comparative study of forward and backward test-kinetic simulation approaches.
Comput. Phys. Commun., 183(12):2561–2569.

Yoshida, H. (1993).
Recent Progress in the Theory and Application of Symplectic Integrators.
Celest. Mech. Dyn. Astron., 56:27–43.

Zenitani, S. and Umeda, T. (2018).
On the Boris solver in particle-in-cell simulation.
Phys. Plasmas, 25(11):112110.

Zhou, X., Büchner, J., Bárta, M., Gan, W., and Liu, S. (2015).
Electron Acceleration By Cascading Reconnection In The Solar Corona. I. Magnetic Gradient And Curvature Drift Effects.
Astrophys. J., 815(1):6.

Zhou, X., Büchner, J., Bárta, M., Gan, W., and Liu, S. (2016).
Electron Acceleration By Cascading Reconnection in the Solar Corona. II. Resistive Electric Field Effects.
Astrophys. J., 827(2):94.

Zhou, X., Büchner, J., Widmer, F., and Muñoz, P. A. (2018).
Electron acceleration by turbulent plasmoid reconnection.
Phys. Plasmas, 25(4):042904.